PHOTOCATHODES IN ACCELERATOR APPLICATIONS* **

J. S. Fraser, R. L. Sheffield, E. R. Gray, P. M. Giles,
R. W. Springer and V. A. Loebs, MS H825
Los Alamos National Laboratory, Los Alamos, NM 87545

Abstract

Some electron accelerator applications require bursts of short pulses at high microscopic repetition rates and high peak brightness. A photocathode, illuminated by a mode locked laser, is well suited to filling this need. The intrinsic brightness of a photoemitter beam is high; experiments are under way at Los Alamos to study the brightness of short bunches with high space charge after acceleration. A laser-illuminated Cs_3Sb photoemitter is located in the first rf cavity of an injector linac. Diagnostics include a pepper pot emittance analyzer, a magnetic spectrometer, and a streak camera.

Introduction

Electron accelerator applications that require a beam of high peak brightness as well as a high pulse repetition rate put severe demands on the electron source and injector. The conventional solution to this problem is to use a pulsed thermionic emitter of low peak brightness followed by a bunching, or phase compression, system that increases the peak current by a large factor. Ideally, the peak brightness should increase in proportion to the bunching factor; in reality, however, the result always falls short of the ideal. An additional shortcoming in the conventional buncher is that a repetition rate in excess of a few tens of megahertz is beyond the state of the art of electronically switching a thermionic triode electron gun. There have been several reports of diode and triode guns operated in an rf cavity to produce electron pulses of width somewhat less than one quarter of the rf period[1-3]. The ultimate upper limit to this technique for triode guns may be the power dissipation in the grid.

In current applications of rf driven free electron lasers, trains of over 300 A, 16 ps wide (5 nC charge) pulses are being used[4]. Recent success[5] with the production of high peak currents from a laser illuminated photocathode shows that high repetition rates in high peak brightness electron beams may be possible. At the Los Alamos National Laboratory, a program is under way to develop a high peak brightness, high average current photoelectron injector.

The Los Alamos Photoinjector Program

In 1985, the achievement of high peak currents from a Cs_3Sb photocathode was reported[5]. It has been shown that the laser driven photocathode produces an intrinsically bright beam[6]. It remains to be demonstrated that short bunches can be accelerated to relativistic energies without loss of brightness. It is evident from simulation studies[7] of the acceleration of short bunches in an rf cavity that dense space charge and the external rf field lead to a degradation of beam quality and, therefore, to a loss of brightness. Although pulses of only a few picoseconds can be produced in a photocathode, it now seems advisable to generate pulses that initially are about 100 ps long and then, after acceleration to about 10 MeV, to bunch them magnetically[8]. Acceleration of the longer bunches is best done in a low frequency linac at a subharmonic of the main linac frequency[9]. Nevertheless, there is a strong incentive to accelerate the bunches as rapidly as possible, a condition that can be met only with high frequency rf fields[10]. A study of the envelope equation in Ref 11 reveals that, for continuous beams, the dominance of space charge over emittance is adiabatically damped as $\gamma^{-1/2}$. A

paper in these proceedings[12] shows that for bunched beams, the damping dependence on energy is much stronger, namely γ^{-2}. Therefore, the requirement of maximum accelerating gradient (hence a high frequency) to minimize the influence of space charge must be balanced against a conflicting need to accept long pulses (hence a low frequency to reduce the emittance growth associated with rf fields).

The conceptual design of a subharmonic injector linac with an rf gun electron source has been described earlier[9]. The initial rf gun experiments, however, are being carried out at a high frequency because a powerful klystron was available for use at 1300 MHz. A schematic diagram of the Los Alamos injector experiment is shown in Fig 1.
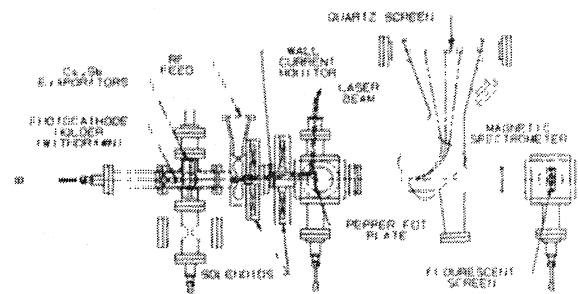

Fig 1 Plan view of the photoinjector experiment

Photocathode Design

In recent years, photocathodes for polarized electron sources have been made from wafers of GaAs[13,14]. Current densities as high as 180 A/cm² have been reported[14]. Photoemitters of Cs_3Sb are less demanding of system cleanliness[15] than are those of GaAs. An additional advantage of a positive electron affinity semiconductor like Cs_3Sb lies in the rapid emission of the photoelectrons[16]. By contrast, the intrinsic emission time uncertainty of GaAs has been measured in the range from 8 to 71 ps for active layers between 50 nm and 2 µm in thickness[16].

A cesium antimonide (Cs_3Sb) photocathode was chosen for its ease of preparation within the vacuum environment of the linac and for its relative tolerance of vacuum conditions in the injector linac[15]. A photoinjector linac must be bakeable in its entirety to about 200°C and be capable of maintaining a pressure below 10^{-9} torr, preferably 10^{-10} torr. If a Cs_3Sb photocathode is damaged in use, the damage can be erased by heating to 400°C, then a new one prepared in situ.

The spectral response[17] of Cs_3Sb extends from a quantum energy of 1.8 eV (λ = 690 nm) to energies greater than 3.8 eV (λ < 320 nm). Therefore, a Cs_3Sb photocathode can be used with a Nd:YAG laser with frequency doubled (λ = 532 nm) or tripled (λ = 355 nm). A Nd:YAG laser can readily be mode locked to deliver trains of 60 ps pulses at a microscopic repetition rate in a range from 50 to 120 MHz.

Rf Gun Cavity Design

The highest possible acceleration rate in the rf gun cavity is limited by the sparking breakdown characteristic of the cavity. A typical rf cavity, optimized for maximum effective shunt impedance Z'^2, will have a ratio of peak surface electric field to average acceleration gradient[10] of about 6. A lower ratio, hence a larger maximum

accelerating field, is obtained by decreasing the curvature of the beam hole nose. Such a cavity is less efficient, but one gains a high acceleration rate with its use.

Jones and Peter[8] have shown that linear radial electric fields in an accelerating cavity lead to a lower emittance growth for beams of uniform space charge density. An rf gun cavity designed for linear radial electric fields automatically has a low ratio of peak surface field to average accelerating field. Therefore, the rf gun cavity was designed to produce linear electric fields, at least in the region traversed by the beam. In the design procedure, the beam hole nose is made an equipotential surface satisfying the equation

$$\rho^2 = 2 \frac{(\psi \quad \zeta)(1 \quad 2\mu) + \zeta^3/3 \quad \mu\zeta^2}{\zeta \quad \mu}$$

where ψ is a chosen potential, $\zeta = z/Z_0$, μ is a focusing parameter, and Z_0 is a scaling parameter. An equipotential is chosen so that a minimum of ψ coincides with the specified beam hole aperture and the scaling parameter Z_0 is equal to half the gap length in the cavity. At radii larger than twice the beam hole radius, the cavity is shaped iteratively using the codes URMEL[18] or SUPERFISH[19] to maximize the effective shunt impedance. A ratio of peak surface field to average accelerating gradient as low as 4 can be achieved while retaining the feature of linearity of the radial electric field.

In the Los Alamos photoinjector, the 1300 MHz cavity design adopted had an effective shunt impedance $ZT^2 = 36$ MΩ/m. With a peak surface field of 60 MV/m (twice the nominal Kilpatrick breakdown field),[20] the average accelerating gradient is 15 9 MeV/m, a ratio of 3 8. The cavity power dissipation under maximum surface field conditions is 0 6 MW.

The rf gun cavity is, of necessity, an asymmetric cavity with the photocathode located on a solid end wall (Fig 2). The shape of the beam hole nose is identical to that of the accelerating cell described above, and the end wall opposite is a member of the same family of equipotential surfaces. The scaling parameter was $Z_0 = 3$ 0 cm and the focusing parameter was $\mu = 0$ 15.
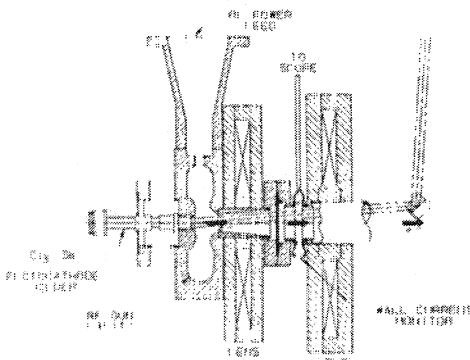

Fig 2 The rf gun cavity

As described below, the photocathode is prepared on a retractable holder. When in the operational position in the rf gun cavity, an effective rf contact must be made between the photocathode holder and the cavity wall. Several experimental models were tested, all incorporating a silver plated spring ring contact. The chosen design reduced the measured Q of a copper test model by less than 2%

Preparation Chamber Design

Initial experiments were carried out with a preparation chamber assembled from commercially available crosses, tees, and nipples (Fig 1). The pumping conductance of this system was limited but adequate for proof of principle tests.

Cesium and antimony evaporators are placed behind a mask with a 1 cm² aperture exposing the photocathode surface. The photocathode is cleaned by heating it to 400°C for one hour. After cooling to 150°C, the alternating deposition of antimony and cesium proceeds. White light is directed onto the photocathode surface with a mirror. The photocathode is insulated from ground by a ceramic support rod so that the photoemission current could be monitored. After maximizing the photoemission, the photocathode is cooled to room temperature, and a final layer of cesium is deposited. In the present preparation chamber, quantum efficiencies of 1 2% are routinely achieved.

The Mode Locked Laser

The quantum energy of the frequency doubled laser output at 532 nm is 2 3 eV. The incident peak laser power required to generate a photocurrent of 1 amperes is

$$P = 2\,31/(\text{quantum efficiency})$$

For a nominal quantum efficiency of 0.01, a current of 200 A requires a peak power of 4.6×10^4 W incident on the photocathode.

The source of light pulses in the present experiment is a cw Nd:YAG laser with a 10 W average power output at 1064 nm (Fig 3). A cavity mode locker driven at 54 166 MHz produces a micropulse train at 108 33 MHz. A Pockels cell gates the pulse train, producing a macropulse burst of up to 20 µs in length at a 1 Hz repetition rate. The macropulse is amplified by two cascaded amplifiers by a variable factor up to 1000, giving a peak output power of up to 1 MW in the micropulses.
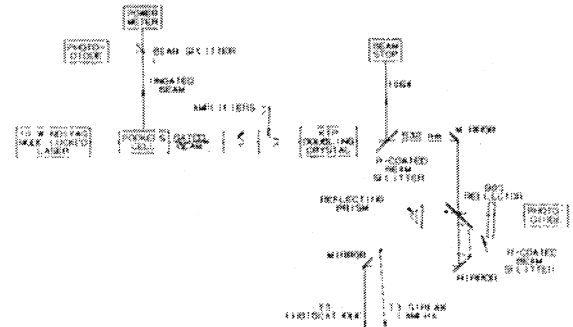

Fig 3 Block diagram of the mode locked laser system

The 1064 nm macropulse beam is focused onto a KTP crystal that halves the wavelength with an efficiency of 50% The emerging green light beam ($\lambda = 532$ nm) is then passed through a filter separating the 532 nm radiation from the 1064 nm radiation.

The green light beam passes through a beam splitter, a 2% fraction being used as a reference for comparison of the temporal profiles of the laser beam and of the rf gun beam in a streak camera (Fig 4).

Finally, an electrically operated shutter, interlocked with a protective gate controlling access to the area, permits transmission of the laser beam into the accelerator enclosure only when the gate is closed and the interlocks cleared.

Diagnostics

After leaving the rf gun cavity, the electron beam passes through two iron shielded solenoid lenses as shown in Figs 1 and 2. Between the two solenoids is a wall current monitor (WCM) of the type used in the SLC
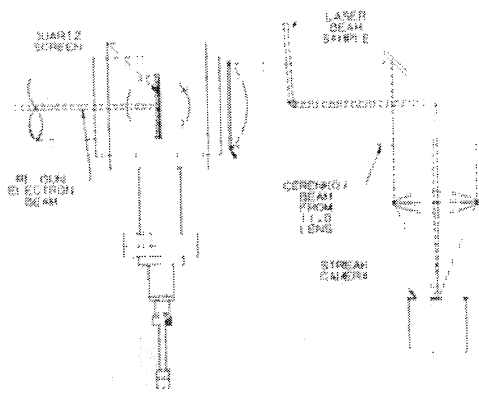
Fig. 4 Temporal profiles of the laser beam and photo electron beam are measured on a single sweep in the streak camera

injector [21] The WCM is loaded with four 51 Ω resistors and a 50 Ω cable leading to an oscilloscope. The monitor was calibrated in a tapered, coaxial, 50 Ω fixture connected to a subnanosecond pulse generator. The central conductor of the fixture is terminated in a 50 Ω resistor The relative pulse amplitudes observed on the WCM output and on the terminating resistor yielded an effective impedance of 8 0 ± 0.1 Ω.

Although the frequencies generated by the beam pulses and the pulser are beyond the band pass of the WCM with its associated external circuit, the integral of the voltage trace observed on the oscilloscope, divided by the WCM impedance, is a valid measure of the bunch (or pulser) charge. This conclusion was verified by measuring the charge in the pulser output with five different detector bandwidths, ranging from 200 MHz to 10 GHz. The measured pulser charge was 130 pC with an rms deviation of 10 pC.

The transverse emittance of the rf gun beam is measured by the pepper pot method [22] In the present experiments, beamlet hole diameters of 127 μm and 1 mm are used The whole beam radius is measured on a quartz plate in the plane of the pepper pot plate When the envelope of the phase space area of a beamlet at the center of the whole beam is plotted on an xx' grid, it intercepts the x' axis at $x' = 1 x'_{int}$. Using the value of the whole beam's maximum radius x_m, the beam emittance is given by $E = \pi x_m x_{int}$ and the normalized emittance by $E_n = \beta \gamma \pi x_m x'_{int}$.

As the beam emerges from the rf gun cavity, it may be focused by one or both of the solenoid lenses The second solenoid can produce a waist at the pepper pot plate for beam currents up to 200 A When only the first lens is used, space charge force forms a waist before the beam reaches the pepper pot This condition, which was verified by integration of the envelope equation for typical beams of 100 to 200 A, is advantageous for the pepper pot method because it ensures that the beamlet propagation from the pepper pot plate to the screen is governed predominantly by emittance, rather than by the upstream focusing force

The temporal profile of the bunches is measured with a streak camera using the Čerenkov radiation from a pure quartz plate (Fig 4) The Čerenkov light is collected by a planoconvex, f 1 0 lens placed in contact with a quartz viewport The collimated light is transported to the streak camera and focused onto the entrance slit with an overall magnification of 1/10 A sample of the laser pulse light is merged with the electron beam's Čerenkov light by a 45° internally reflecting prism in the middle of the

Čerenkov light beam, thereby eliminating the trigger jitter in the streak camera The streak camera sweep speed was calibrated using a variable path length for the laser light created by a movable retroreflector on an optical bench

A double focusing magnetic spectrometer is installed on the beamline The dispersion on the detector plane is 0 8 cm%, and the magnification is unity With the aid of the two solenoid lenses, a 20% momentum band can be analyzed Alternatively, a 127 μm diam hole can be scanned across a beam diameter at the object position (the pepper pot plate) to do a differential momentum analysis For this purpose, an intensified vidicon can view the detector plane through one of two viewports available.

Experimental Results

Initial observation of the accelerated electron beam from the rf gun was obtained with the WCM (Fig 5) With a fast oscilloscope, the largest pulse trains repeatedly observed had peak amplitudes of 4 4 V with 40 dB of attenuation in place The measured bunch charge, obtained from the integrated pulse profiles, was 27 nC, giving an average current in the pulse train of 2 9 A Assuming that the temporal profile was Gaussian (see below), the peak current was 390 A The probable error in these measurements is ± 20%

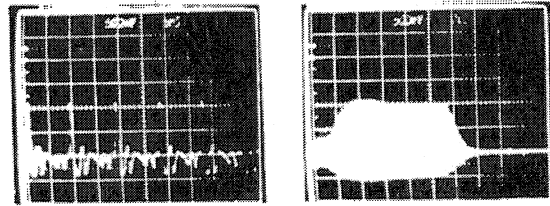Fig 5. Wall current monitor traces of pulse trains at 108 3 MHz, (a) at 5 ns/div and (b) 2 ps/div

The minimum laser pulse width observed was 53 ± 1 ps FWHM; on the same streak camera sweep, the electron bunch widths were the same to within the experimental error (Fig 6) when allowance is made for the observed 6% energy spread We conclude, therefore, that for the present experimental conditions, the pulse broadening introduced by the Cs_3Sb photoemission is less than 10 ps

The emittance of space charge dominated beams was measured with peak currents ranging from 100 to 150 A Fig 7 shows a pepper pot pattern on a quartz screen 92 cm from a tantalum plate drilled with 127 μm diam holes on 2 mm centers Figure 7(b) is a cut through one line of spots The equivalent spacing between grid lines is 7 8 mm The measured point spreading from the Čerenkov cone angle is 0 7 mm Four measurement sets were made under various combinations of peak current and focusing strength in the first solenoid (Table I). The average normalized emittance for the four sets is 20 π mm mrad The corresponding normalized peak brightness is 4 2 × 10^10 A/(m² rad²) and the average macropulse current is 1 0 A The estimated probable error on all these measurements is ± 20%. No corrections have been made for space charge effects In the fourth set in Table I, the photoemitter current density is estimated to be 600 A/cm² from measurements of the laser beam area and the peak current The beam energy measured on the double focusing spectrometer agreed within 10% of the predicted value, 1 1 MeV The measured energy spread was ± 3%

GAUSSIAN FIT OF LASER PULSE
SIGMA = 21.9 +/- 0.2 ps

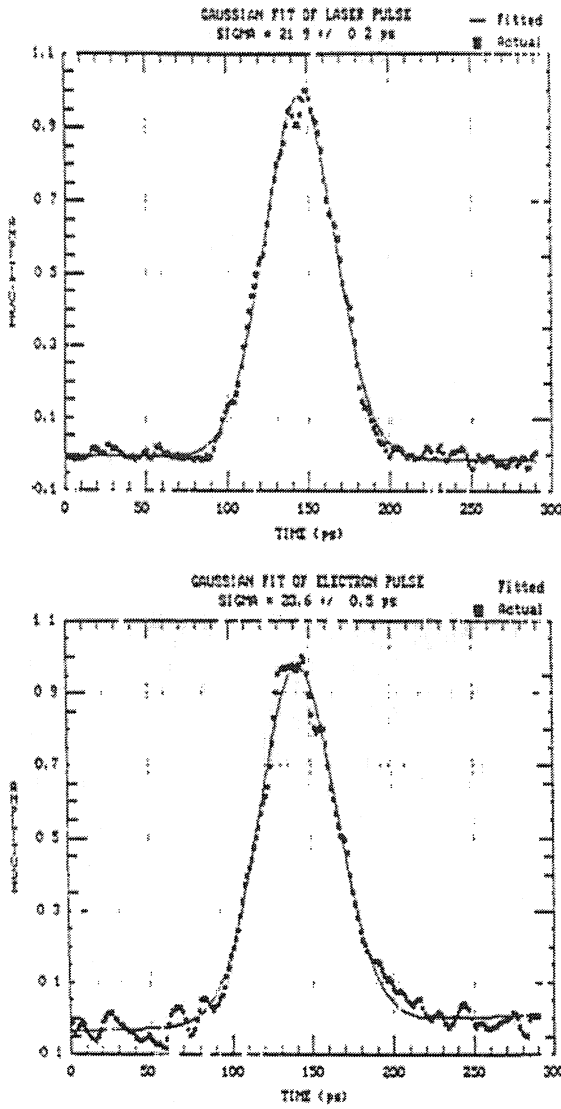GAUSSIAN FIT OF ELECTRON PULSE
SIGMA = 23.6 +/- 0.5 ps

Fig 6 Digitized streak camera temporal profiles of the laser and photoinjector beams
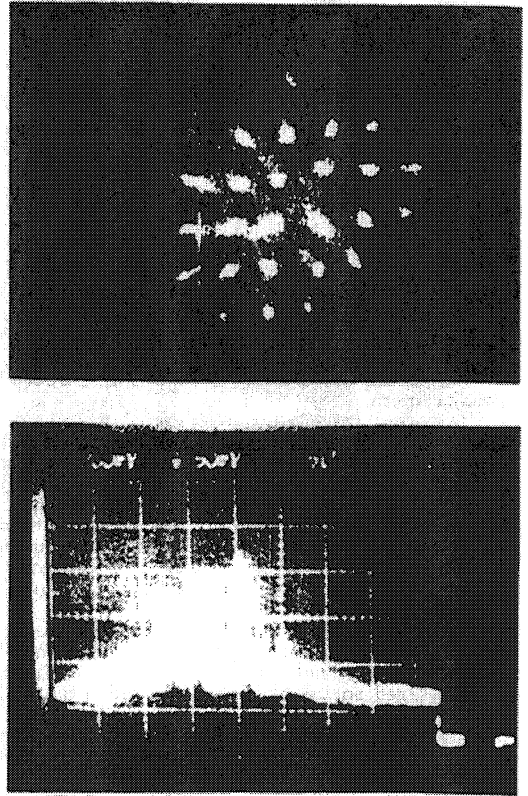

Fig. 7. (a) Pepper pot image 92 cm from a tantalum plate with 1217 μm diam holes on 2 mm centers; (b) a cut through one row of spots; the horizontal scale is 7.8 mm per 5 μs

TABLE I
EMITTANCE MEASUREMENTS

Set	Peak Current (A)	Lens 1 Current (A)	Bunch Charge (nC)	X_m (mm)	X'_{int} (mrad)	Normalized Emittance ($\beta\gamma = 3.0$) (π mm mrad)	Normalized Brightness (A/m² rad²)
1	100	235	8	3.9	1.7	20	2.5×10^{10}
2	150	310	12	7.5	1.4	32	1.4×10^{10}
3	130	314	10	3.9	1.5	18	4×10^{10}
4	100	320	8	5.1	0.7	11	9×10^{10}

Conclusions

The photoinjector experiment demonstrated the predicted performance in yield and temporal response and exceeded expectations in current density and brightness. The temporal profile measurements prove that the emission time uncertainty for Cs_3Sb photoemission is less that 10 ps

Acknowledgments

References

1. S. P. Kapitza and V. N. Melekhin, *The Microtron*, Harwood Academic Publishers, London, 1978, p. 112.

2. D. E. Poole, T. R. Charlesworth, O. Gunnill, D. G. Peters, and G. Saxon, "An RF Modulated Electron Gun for NINA Injection Equipment," IEEE Trans Nucl Sci 20 (3), 399 (1973)

3. G. A. Westenkow and J. M. J. Madey, "Microwave Electron Gun," Lasers and Particle Beams 2, 223 (1984).

4. R. W. Warren, D. W. Feldman, B. E. Newnam, S. C. Bender, W. E. Stein, A. H. Lumpkin, R. A. Lohsen, J. C. Goldstein, B. D. McVey, and K. C. D. Chan, "Recent Results From The Los Alamos Free Electron Laser," Proc 8th Int. Free Electron Laser Conf., Glasgow, Sept. 1986, Los Alamos National Laboratory document LA UR 86 3009, to be published.

5. C. H. Lee, P. E. Oettinger, E. R. Pugh, R. Klinkowstein, J. H. Jacob, J. S. Fraser, and R. L. Sheffield, "Electron Emission of Over 200 A/cm² From a Pulsed Laser Irradiated Photocathode," IEEE Trans Nucl. Sci 32 (5), 3045 (1985)

6. P. E. Oettinger, I. Bursuc, R. E. Shefer, and E. R. Pugh, "Brightness of an Intense Electron Beam Generated by a Pulse Laser Irradiated Photocathode," these proceedings

7. M. E. Jones and W. K. Peter, "Particle in Cell Simulations of the Lasertron," IEEE Trans Nucl Sci. 32 (5), 1794 (1985).

8. M. E. Jones and W. K. Peter, "Theory and Simulation of High Brightness Electron Beam Production From Laser Irradiated Photocathodes in the Presence of DC and RF Electric Fields," Proc 6th Int Conf. on High Power Particle Beams, Kobe, Japan, 1986, to be published

9. J. S. Fraser, "Electron Linac Injector Developments," Proc 1986 Linear Accelerator Conf., Stanford Linear Accelerator Center report SLAC 303, 411 (1986).

10. S. O. Schriber, "Factors Limiting the Operation of Structures Under High Gradient," Proc. 1986 Linear Accelerator Conf, Stanford Linear Accelerator Center report SLAC 303, 591 (1986)

11. J. D. Lawson, *The Physics of Charged Particle Beams*, Oxford University Press, Oxford, 1977, p. 134

12. M. E. Jones and B. E. Carlsten, "Space Charge Induced Emittance Growth in the Transport of High Brightness Electron Beams," these proceedings.

13. D. T. Pierce, R. J. Celotta, G. C. Wang, W. N. Unertl, A. Galens, C. E. Kuyatt, and S. R. Mielczarek, "GaAs Spin Polarized Electron Source," Rev Sci Inst 51, 478 (1980).

14. C. K. Sinclair and R. H. Miller, "A High Current, Short Pulse, RF Synchronized Electron Source for the Stanford Linear Collider," IEEE Trans Nucl Sci 28, (3), 2649 (1981).

15. C. H. Lee, P. E. Oettinger, A. Sliski, and M. Fishbein, "Practical Laser Activated Photo emissive Electron Source," Rev Sci Instrum. 56, 560 (1985)

16. C. C. Phillips, A. E. Hughes, and W. Sibbett, "Photochron Streak Camera with GaAs Photocathode," in *Ultrafast Phenomena IV*, Eds., D. H. Auston and K. W. B. Eisenthal, Springer Verlag, Berlin, 1984, p. 420

17. W. E. Spicer, "Photoemissive, Photoconductive, and Optical Absorption Studies of Alkali Antimonide Compounds," Phys. Rev 112, 114 (1958)

18. T. Weiland, "TBCI and URMEL New Computer Codes for Wake Field and Cavity Mode Calculations," IEEE Trans. Nucl Sci 30 (4), 2489 (1983).

19. K. Halbach, R. F. Holsinger, W. E. Jule, and D. A. Swenson, "Properties of the Cylindrical RF Cavity Evaluation Code SUPERFISH," Proc 1976 Proton Linear Accelerator Conf, AECL 5677, 122 (1976)

20. W. D. Kilpatrick, "Criterion for Sparking Designed to Include Both RF and DC," Rev Sci Instrum, 28, 824 (1957)

21. M. B. James, J. E. Clendenin, S. D. Ecklund, R. H. Miller, J. C. Sheppard, C. K. Sinclair, and J. Sodja, "Update on the High Current Injector for the Stanford Linear Collider," IEEE Trans Nucl Sci 30 (4), 2992 (1983)

22. C. LeJeune and J. Aubert, "Emittance and Brightness: Definitions and Measurements," in *Applied Charged Particle Optics*, Ed, A. Septier, Advances in Electronics and Electron Phys, Supp 13A (1980)

*   *   *

Discussion

H. Henke, CERN

What are time of flight, pulse length and energy spread?

Reply

Many more details are given in the paper. The overall pulse length is 10 μs, during which electrons are provided in 60 ps bunches at 108 MHz, the 12th subharmonic of the rf cavity frequency. The quoted energy spread is ±3%; this is within 10% of the expected value for the 1 MeV output beam.